1

Seagrass rhizosphere microenvironment alters plant-associated microbial community composition

4

5 Kasper Elgetti Brodersen[1,2,*], Nachshon Siboni[1], Daniel A. Nielsen[1], Mathieu
6 Pernice[1], Peter J. Ralph[1], Justin Seymour[1], Michael Kühl[1,2]

7

8 [1]Climate Change Cluster, Faculty of Science, University of Technology Sydney (UTS), Sydney,
9 NSW, Australia.

10 [2]Marine Biological Section, Department of Biology, University of Copenhagen, Helsingør,
11 Denmark.

12

13 *Running title*: "Seagrass rhizosphere microbes".

14

15 *Corresponding author: Kasper Elgetti Brodersen, email: kasper.elgetti.brodersen@bio.ku.dk
16 and phone: + 45 9176 8585.

17

18 <u>Originality-Significance Statement:</u>

19 Seagrasses actively select for a distinct microbial community composition at the
20 plant/sediment interface, which may positively affect the nutrient availability in the seagrass
21 rhizosphere owing to enhanced nitrogen fixation by sulphate-reducing, diazotrophic bacteria.
22 We provide evidence of a potential mutualistic beneficial relationship between seagrasses
23 and rhizospheric, heterotrophic diazotrophs based on a mutual exchange of essential
24 nutrients.

25

26

27 MAIN BODY: 4.593 words

28 **SUMMARY**

29 The seagrass rhizosphere harbors dynamic microenvironments, where plant-driven gradients

30 of O_2 and dissolved organic carbon form microhabitats that select for distinct microbial

31 communities. To examine how seagrass-mediated alterations of rhizosphere geochemistry

32 affect microbial communities at the microscale level, we applied 16S rRNA amplicon

33 sequencing of artificial sediments surrounding the meristematic tissues of the seagrass

34 *Zostera muelleri* together with microsensor measurements of the chemical conditions at the

35 basal leaf meristem (BLM). Radial O_2 loss (ROL) from the BLM led to ~300 µm thick oxic

36 microzones, wherein pronounced decreases in H_2S and pH occurred. Significantly higher

37 relative abundances of sulphate-reducing bacteria were observed around the meristematic

38 tissues compared to the bulk sediment, especially around the root apical meristems (RAM;

39 ~57% of sequences). Within oxic microniches, elevated abundances of sulphide-oxidizing

40 bacteria were observed compared to the bulk sediment and around the RAM. However,

41 sulphide oxidisers within the oxic microzone did not enhance sediment detoxification, as rates

42 of H_2S re-oxidation here were similar to those observed in a pre-sterilized root/rhizome

43 environment. Our results provide novel insights into how chemical and microbiological

44 processes in the seagrass rhizosphere modulate plant-microbe interactions potentially

45 affecting seagrass health.

46

49

50

Introduction

Seagrass meadows are high-value ecosystems (Costanza et al. 1997) that provide numerous ecosystem services to marine environments, such as facilitating nursery areas for many juvenile fish and crustaceans (Harborne et al. 2006; Larkum et al. 2006), improving water quality through increased sedimentation (Ward et al. 1984; Madsen et al. 2001), providing a main food source for iconic marine animals such as sea turtles and dugongs, and a high ability to sequester carbon in the sediment (Duarte et al. 2005; Fourqurean et al. 2012). Seagrass ecosystems harbour a unique microbiome including populations of microbes attached to seagrass leaves and within the rhizosphere, with microorganisms involved in the sulphur cycle known to play particularly important functional roles (e.g. Devereux, 2005; Jensen et al. 2007; Cúcio et al. 2016; Fahimipour et al. 2017). However, a quantitative understanding of the importance of this microbiome on the fitness of seagrass plants is lacking (York et al. 2016). Jensen et al. (2007) showed that sulphate-reducing bacteria (SRB) and sulphide-oxidizing bacteria (SOB) are located in different microniches within the seagrass rhizosphere, with their distributions largely defined by rhizospheric O_2 availability, and the authors suggested that SOB may be beneficial to seagrasses by removing toxic H_2S from the rhizosphere. However, this hypothesis was derived from bulk sample analysis and did not include measurements of H_2S oxidation within oxic microniches harbouring SOB. To truly tease apart the relationships between seagrasses and communities of SRB and SOB there is thus a need for combined microbiological and biogeochemical characterization of the seagrass rhizosphere microenvironment.

Seagrasses grow in largely anoxic, reduced marine sediments (Borum et al. 2005) that are often enriched in the potent phytotoxin H_2S (Holmer et al. 2006; van der Heide et al. 2012; Lamers et al. 2013). These anoxic and sulphidic conditions are a consequence of the deposition of large amounts of organic matter in seagrass meadows driving microbial remineralization processes, which are dominated by SRB (Jørgensen, 1982; Blaabjerg & Finster, 1998; Blaabjerg et al. 1998; Nielsen et al. 2001). To accommodate growth in such hostile environments, seagrasses release O_2 into their rhizosphere, *i.e.,* the small volume of sediment directly influenced by root/rhizome secretions and associated microbes, from their basal leaf meristem and root apical meristems. This so-called radial O_2 loss (ROL), leads to the formation of localised oxic microniches around the seagrass roots/rhizome (Pedersen et al.

82   1998; Jensen et al. 2005; Brodersen et al. 2015a; Koren et al. 2015; Brodersen et al. 2016).

83   These plant-driven oxic microzones support local H_2S re-oxidation and thereby protect the

84   most vulnerable parts of the plants against the H_2S produced by SRB in the surrounding anoxic

85   sediments (Brodersen et al. 2015a). While oxic microniches form mainly around growing root

86   tissues, mature regions of the roots possess physical barriers to ROL, which are typically

87   composed of Casparian-band like structures that may function as an analogous barrier to H_2S

88   intrusion (Barnabas, 1996; Colmer, 2003). Seagrass rhizomes and roots also release significant

89   amounts of labile dissolved organic carbon (DOC), especially around the root-cap (Moriarty

90   et al. 1986; Pollard & Moriarty, 1991), which can stimulate microbial activity including

91   sulphate reduction in the rhizosphere (Isaksen & Finster, 1996; Blaabjerg et al. 1998; Hansen

92   et al. 2000; Nielsen et al. 2001). Seagrasses thus substantially alter the biogeochemical

93   conditions within their rhizosphere, resulting in a dynamic mosaic of chemical microgradients

94   that influence both the distribution and activity of the plant-associated microbial community

95   (Devereux, 2005; Jensen et al. 2007; Brodersen et al. 2015a; Brodersen et al. 2016; Cúcio et

96   al. 2016).

97

98   Seagrass-driven modulation of the rhizosphere microhabitat has been suggested to initiate

99   mutualistic relationships between seagrasses and diazotrophic SRB based on reciprocal

100   nutrient exchange, whereby the seagrass host provides a carbon source to the diazotrophs

101   that in return fix dinitrogen (Hansen et al. 2000; Welsh et al. 2000; Nielsen et al. 2001).

102   Sulphide-oxidizing bacteria within oxic microenvironments in the rhizosphere have also been

103   proposed to play an important role in sediment detoxification (Jensen et al. 2007; Cúcio et al.

104   2016; Fahimipour et al. 2017). Bacterial-mediated H_2S oxidation is 10^4-10^5 times faster than

105   spontaneous chemical oxidation (Jørgensen & Revsbech, 1983; Nelson et al. 1986) and given

106   ample O_2 supply, SOB may thus efficiently remove toxic H_2S, facilitating seagrass colonization

107   of highly sulfidic sediments. However, technical constraints in examining the distribution and

108   activity of bacteria at the appropriate microscale resolution and at specific plant-driven

109   chemical micro-hotspots have prevented confirmation of a beneficial role of SOB within the

110   seagrass rhizosphere.

111   Here we present a detailed description of the microbial diversity surrounding the

112   meristematic tissues of *Z. muelleri* in combination with measurements of plant-modulated

113   chemical micro-habitats in the seagrass rhizosphere, with the aim of elucidating the potential

114   importance of SOB in detoxifying sediments for seagrasses, relative to plant-derived

115   spontaneous chemical re-oxidation with O_2.

116

Results and discussion

The seagrass rhizosphere is dominated by bacteria involved in the sediment sulphur cycle (Jensen et al. 2007; Cúcio et al. 2016), but little is known about whether they alleviate or aggravate the exposure of below-ground seagrass biomass to phytotoxic H_2S. This lack of knowledge is particularly significant for the vital meristematic regions of the plants that lack barriers to ROL and are thereby most likely to experience H_2S intrusion (Colmer, 2003). However, this would only occur when ROL is insufficient to re-oxidize sulphide diffusing towards the below-ground tissue surface, as seen during severe events of water-column hypoxia in darkness (Brodersen et al., 2015a). Overall, the ROL-driven oxic microshields are understood as providing better protection of the below-ground tissues as they prevent phytotoxic sulphide from reaching the tissue surface (Koren et al. 2015; Brodersen et al. 2015a; Brodersen et al. 2017). Instead, the relatively impermeable mature parts of the below-ground tissues likely improve long-distance, internal transport of O_2 from leaves to distal root-tips (Colmer, 2003; Pedersen et al. 2004; Borum et al. 2006). Here, we combined detailed microscale measurements of the geochemical conditions and dynamics in the seagrass rhizosphere with analysis of the microbial community composition to determine, whether seagrasses benefit from rhizospheric bacterial-mediated sulphide oxidation. We focused on the small volume of sediment surrounding the meristematic regions of the plant, as this part of the seagrass rhizosphere is most significantly affected by the seagrass host and exhibits strong chemical microgradients of O_2 and DOC availability (Moriarty et al. 1986; Pedersen et al. 1998; Jensen et al. 2007; Brodersen et al. 2015a). We were able to detect changes in the microbial community composition as a response to the activity of the seagrass host, without disturbing the below-ground biogeochemical micro-gradients and habitats during microsensor measurements, and determined that SOB are playing an important role in H_2S oxidation in the seagrass rhizosphere.

Dynamics of the below-ground chemical microenvironment

Radial O_2 loss (ROL) from the basal leaf meristem led to a ~300 µm thick oxic microzone, protecting seagrasses from intrusion of H_2S through chemical oxidation at the oxic/anoxic interface (Fig. 1; Fig. S1 and S2; Table 1). In light, the O_2 efflux amounted to ~745 nmol O_2 cm⁻

147 ^{2} h^{-1} compared to ~322 nmol O_2 cm^{-2} h^{-1} in darkness in the microbe-enriched treatment (Table

148 1). In the pre-sterilized environment, ROL also increased more than 2-fold in the light,

149 resulting in an O_2 efflux of ~891 nmol O_2 cm^{-2} h^{-1}, compared to ~378 nmol O_2 cm^{-2} h^{-1} in

150 darkness (Table 1). The enhanced ROL from the below-ground tissue during light stimulation

151 of the leaf canopy resulted in a slightly enhanced thickness of the rhizospheric oxic microzone

152 by ~50 µm in both treatments (Fig. 1).

153 At the plant-driven rhizospheric oxic/anoxic interface (*i.e.*, the dotted line on Fig. 1 ~300 µm

154 from the tissue surface), we found a rapid decrease in sediment H_2S concentrations from ~100

155 µmol L^{-1} at ~1 mm away from the below-ground tissue surface to 0 µmol L^{-1} at the oxic/anoxic

156 interface or slightly within the oxic microzone (Fig. 1; Fig. S1 and S2); thus showing complete

157 detoxification of sedimentary H_2S before reaching the tissue surface. The ratio between the

158 O_2 and total sulphide fluxes, *i.e.*, the amount of O_2 molecules released from the below-ground

159 tissue compared to the total amount of sulphide (H_2S, HS^- and S^{2-}) oxidized at the basal leaf

160 meristem in the artificial sediment was 0.6 in darkness and 1.7 in light for both treatments

161 (Table 1). This is indicative of incomplete H_2S oxidation to elemental sulphur (S^0) in the dark

162 (the stoichiometry of sulphide oxidation to S^0 is: $0.5O_2 \rightarrow S^0$; Nielsen et al. 2006) and complete

163 H_2S re-oxidation to sulphuric acid (H_2SO_4) in the light (stoichiometry of 2:1). Alternatively, the

164 higher O_2 flux in the light could indicate higher microbial O_2 consumption rates and/or

165 chemical oxidation of other reduced compounds, such as Fe^{2+}, within the rhizosphere. Or that

166 some of the rhizosphere sulphide (S_{tot}^{2-}) precipitated as FeS during darkness, which would

167 also explain the lower degree of co-existence between O_2 and H_2S in the seagrass rhizosphere

168 in darkness as compared to in light (seen on Fig. 1).This is in accordance with a recent study

169 (Brodersen et al. 2017) that demonstrated Fe^{3+} reduction, and thus Fe^{2+} mobilisation, in the

170 seagrass rhizosphere predominantly during night-time (Brodersen et al. 2017). Moreover, at

171 the seagrass-driven rhizospheric oxic/anoxic interface we also observed a rapid decrease in

172 rhizosphere pH by ~2 pH units (Fig. 1; Fig. S1 and S2), most likely as a result of protons

173 generated from the chemical reaction between O_2 and H_2S (Nielsen et al. 2006; Brodersen et

174 al. 2015a; 2016). This resulted in acidification of the rhizospheric oxic microniches reaching

175 pH 4-5 (Fig. 1).

176

177   *Microbial diversity in the seagrass rhizosphere*

178   The microbial community composition in the artificial sediment was similar to that reported

179   from other seagrass-vegetated natural sediments (e.g. Jensen et al. 2007; Cúcio et al. 2016);

180   with many members of the rhizospheric microbial community affiliated with the sulphur cycle

181   (Cúcio et al. 2016; Ettinger et al. 2017; Fahimipour et al. 2017). Compared to the bulk

182   sediment, we observed higher mean relative abundance of SRB taxa including OTUs matching

183   *Desulfovibrio* sp., especially around the root apical meristems, where members of the SRB

184   class *Clostridia* (Devereux, 2005; Sallam & Steinbüchel, 2009) dominated, with ~57% of

185   sequences affiliated with this bacterial class ($t(5)_{RAM-BS}$=4.015, p=0.01; $t(4)_{RAM-NC}$=16.944,

186   p<0.001; Fig. 2). This is notable given that many members of this class are also known to be

187   diazotrophs, i.e., N_2 fixing SRB. It has previously been argued that diazotrophic bacteria (e.g.

188   *Lachnospiraceae* & *Desulfovibrio* sp.) live in a mutualistic relationship around the below-

189   ground biomass of seagrasses (e.g. Welsh, 2000), where the plant provides DOC and

190   diazotrophic SRB reciprocally provide fixed nitrogen to the seagrass. Nielsen *et al*. (2001), for

191   example, showed higher rates of N_2-fixation and sulphate reduction around and on below-

192   ground tissues of seagrasses as compared to those in the sediment, and that root/rhizome

193   associated SRB fix more dinitrogen than needed for their own growth. In addition, the

194   occurrence of SRB within the rhizosphere may also lead to increased phosphorus

195   solubilisation owing to reduction of insoluble Fe^{3+} oxyhydroxides that can promote the

196   release of previously adsorbed phosphate to the pore-water (Pagès et al. 2011, 2012;

197   Brodersen et al. 2017).

198   Within the plant-derived oxic microzone in the microbe-enriched treatment, sulphide-

199   oxidizing *Epsilonproteobacteria*, including *Arcobacter* sp. and *Sulfurimonas* sp., were detected

200   (Fig. 2). *Epsilonproteobacteria* constituted ~34% of the community at the basal leaf meristem

201   compared to other designated bacterial classes (including *Deltaproteobacteria*, *Clostridia* and

202   *Bacteroidia*), with a relative increase of ~22% as compared to around the root apical

203   meristems (Fig. 2). However, the higher abundance of SOB within plant-derived oxic

204   microniches did not seem to enhance sulphide detoxification, as we observed similar H_2S re-

205   oxidation rates within the pre-sterilized and microbe-enriched treatments (Fig. 1-2; Table 1);

206   which was also shown in calculated rates of total sulphide oxidation (Fig. S3 and S4; Table 1).

207 Spontaneous chemical H_2S re-oxidation via ROL thus seemed of similar magnitude as
208 biological H_2S re-oxidation (Fig. 1; Table 1). However, the mere presence of high populations
209 of SOB indicate that they are playing an important role in H_2S oxidation in the seagrass
210 rhizosphere.

211 Within the seagrass-derived rhizospheric low-pH microniches (corresponding to the oxic
212 microzones; Fig. 1), we observed a slightly lower mean relative abundance of Bacteroidia
213 (~13%) as compared to the root apical meristems and the bulk sediment (>23%) albeit not
214 significant for the porewater enriched sediment ($t(4)_{BLM-RAM}$=-1.141, p>0.05; $t(5)_{BLM-BS}$=-0.461,
215 p>0.05; $t(4)_{BLM-NC}$=-7.894, p=0.001; Fig. 2). The growth rate of *Bacteroidetes* is pH dependent
216 (Thomas et al. 2011), and the potentially impeded growth of these potential plant pathogens
217 (Fig. 2) as a result of reductions in rhizosphere pH driven by ROL from the below-ground
218 tissues (Fig. 1) deserves further attention.

219 Sulphate reduction thus seemed to be the microbial metabolism in the seagrass rhizosphere
220 that was most strongly affected by the activity of the seagrass host, where locally enhanced
221 DOC, especially at the root-tips of seagrasses (Moriarty et al. 1986; Pollard & Moriarty, 1991),
222 could be responsible for the microbial community composition shift (Fig. 2; Fig. S5). The
223 higher relative abundance of the SRB class *Clostridia* at the root apical meristems is supportive
224 of a potential mutualistic relationship between seagrasses and heterotrophic, diazotrophic
225 bacteria based on reciprocal nutrient exchange.

226

227 *Methodology*

228 Our novel experimental approach allowed the combined use of molecular and microsensor
229 techniques, without disturbing the below-ground biogeochemical microenvironment during
230 detailed O_2, H_2S and pH microsensor measurements. Detailed information about the chemical
231 microgradients around the below-ground tissues provided by the microsensor measurements
232 enabled us to sample sediment within only the plant-affected regions of the seagrass
233 rhizosphere. While many modern 'omics' studies are often carried out "blindfolded" by
234 relying on bulk sample analysis, the combination of sampling with microenvironmental

235 analyses, such as described in this study, may alleviate such limitations and guide more

236 hypothesis-driven approaches.

237

238 Some of the limitations of using an artificial sediment matrix mainly relate to it being a

239 simplification of complex natural sediments, where other elements and especially solid-phase

240 species (such as Fe^{3+} oxyhydroxides) also play important roles for reactions affecting

241 distributions of O_2, sulphide and pH in the seagrass rhizosphere (Brodersen et al. 2017).

242 Insoluble Fe^{3+} oxyhydroxides are e.g. likely to accumulate in the seagrass rhizosphere during

243 day-time as a result of chemical and biological oxidation of dissolved Fe^{2+} and precipitated

244 FeS (Brodersen et al. 2017). At night-time, on the other hand, precipitated Fe^{3+} oxyhydroxides

245 are reduced via sulphide, which re-generates dissolved Fe^{2+} leading to consumption of

246 sulphide through precipitation of FeS (Brodersen et al. 2017). Hence, sulphide and O_2

247 consumption processes are more complex in natural sediments as compared to in artificial

248 sediment. Different processes can also be temporally separated, where H_2S consumption at

249 night is in part a result of ROL-driven Fe^{3+} formation during the day, and O_2 consumption in

250 the day is partially due to re-oxidation of FeS, that precipitated in the seagrass rhizosphere

251 during darkness, to regenerate insoluble Fe^{3+} oxyhydroxides (Brodersen et al. 2017).

252

253 *Conclusions*

254 The novel combination of measuring microscale patterns in microbial diversity and sediment

255 chemical characteristics within an artificial sediment matrix showed that seagrass-mediated

256 alterations of rhizosphere geochemistry result in pronounced shifts of the rhizosphere

257 microbial community composition. ROL from the basal leaf meristem resulted in a marked

258 decrease in sediment pH and H_2S concentrations at the plant-driven oxic/anoxic interface,

259 and within the plant-derived oxic microzones, H_2S was completely re-oxidized, protecting the

260 most vulnerable part of the plant against phytotoxic H_2S intrusion. We observed significantly

261 elevated abundances of SRB in the seagrass rhizosphere, and presence of SOB within oxic

262 microniches. Our high-resolution characterization of rhizosphere chemistry and microbial

263 communities indicate that SOB can play an important role for H_2S oxidation in the seagrass

264 rhizosphere, especially within seagrass-generated oxic microniches.

265

266

267 **Experimental procedures**

268 *Seagrass specimens and sediment sampling*

269 Specimens of *Zostera muelleri* subsp. *capricorni* (Asch.) S.W.L. Jacobs and marine sediment

270 were collected from shallow waters (<2 m depth) in a dense seagrass meadow in Narrabeen

271 Lagoon, NSW, Australia (-33.72°S, 151.29°E). Seagrass sediment was collected with open-

272 barrel, push cores (PVC pipe, 25 cm length, 7 cm internal diameter) as described previously

273 (*e.g.* Wesley, 2009). After sampling, the sediment and seagrass samples were transported to

274 a greenhouse facility at University of Technology Sydney, where they were kept under natural

275 sunlight in large, aerated and temperature-controlled seawater reservoirs (temperature of

276 ~22°C; salinity of ~34) before further treatments. Prior to experiments, selected seagrass

277 specimens were gently uprooted and washed free of any adhering sediment particles.

278

279 *Experimental setup*

280 To enable the examination of microscale gradients in chemical and microbiological properties

281 near to and at the seagrass below-ground tissue surface, we employed a novel artificial

282 sediment system consisting of a custom-made split flow-chamber, wherein the investigated

283 seagrass specimens were grown in a transparent, artificial sediment matrix (Brodersen et al.

284 2014). Selected seagrass specimens (one plant at a time) were maintained in the flow-

285 chamber with the leaf canopy positioned in the aerated, free-flowing seawater compartment

286 and the below-ground biomass embedded in a reduced, deoxygenated agar matrix in the

287 adjoining "sediment" compartment. A detailed description of the casting procedure and

288 chemical characteristics of the artificial sediment is given below.

289 A water pump submerged into an aerated and temperature-controlled seawater bath

290 (temperature of ~22°C; Salinity of ~34) provided a constant flow (~0.5 cm s^{-1}) of aerated

291 seawater to the water compartment of the flow chamber. Within the sediment compartment,

292 a ~3 cm-thick anoxic and HEPES buffered (10 mM) water layer, residing above the artificial

293 sediment matrix, functioned as a liquid-phase diffusional barrier to O_2 invasion into the

294 artificial sediment (Brodersen et al. 2014). The anoxic water layer was constantly flushed with

295 humidified N_2 throughout the seagrass cultivation period. Below the artificial sediment

296 matrix, pieces of gauze, pre-soaked in an acidic (pH 4) and anoxic 1 mM Na_2S solution, were

297 deployed to ensure a continuous supply of H_2S to the overlaying artificial sediment matrix.

298   Finally, the sediment compartment was covered with aluminum foil to avoid incoming stray

299   light, retain N_2 and thus limit O_2 intrusion into the anoxic water layer.

300

301   Light was provided as a 12h:12h light/dark cycle with a fiber-optic tungsten halogen lamp (KL-

302   2500; Schott GmbH, Mainz, Germany) connected to a timer and equipped with a collimating

303   lens to restrict the illumination to the leaf canopy only. The incident photon scalar irradiance

304   (PAR, 400-700 nm) at the leaf canopy during cultivation was ~150 µmol photons $m^{-2}\,s^{-1}$. Scalar

305   photon irradiance was measured with a spherical photon irradiance sensor (Walz GmbH,

306   Effeltrich, Germany) connected to a calibrated photon irradiance meter (LI-250A, LiCor,

307   Lincoln, NE, USA).

308

309   *Seagrass cultivation period*

310   Seagrass specimens were generally allowed 2 weeks to recover from sampling and to

311   acclimatize to experimental conditions (temperature and salinity) before cultured in the

312   reduced, transparent artificial sediment. Each experiment ran for a total of 8 days, where (*i*)

313   pulse amplitude modulated (PAM) measurements were performed on the 4th and the second

314   last day (7th) of the experiment, (*ii*) microsensor measurements on the 5th to the 7th day of the

315   experiment, and (*iii*) sediment samples for 16S rRNA amplicon sequencing were taken on the

316   last day (8th) of the experiment, just after the microsensor and PAM measurements. To avoid

317   effects of seasonal changes (such as temperature and nutrient availability) on the sediment

318   microbial community composition, three plant replicates were chosen per treatment (giving

319   a total of 48 experimental days). This is a minor limitation of the methodology, *i.e.,* when

320   combining microsensor profiling with molecular techniques, as determining the chemical

321   microenvironment around below-ground tissues in the casted artificial sediment in high

322   spatio-temporal resolution is a time-consuming process.

323

324   *Artificial sediment matrix in the sediment compartment*

325   To enable identification of potential mutual beneficial relationships between seagrasses and

326   SOB, two treatments were applied, whereby the artificial sediment matrix was either (i)

327   sterilized, including the below-ground biomass surface (negative control), or (ii) enriched with

328   native pore water microbes. Each procedure is explained further in the following paragraphs.

329

i)   Artificial sediment with pore water microbes

330

The transparent, reduced artificial sediment consisted of a ~0.7% (w/v) deoxygenated

331

agar/seawater solution, buffered with an anoxic solution of HEPES buffer (final concentration

332

of 10 mM; pH ~7), and amended with Na_2S (final H_2S concentration of 500 µM; at pH 7) and

333

pore-water microbes (~50% pore-water in the final 0.7% w/v solution). During casting of the

334

artificial sediment with pore-water microbes, the pore-water was homogenously

335

incorporated into the pre-heated agar/seawater solution (~1.4% w/v) shortly before the

336

artificial sediment matrix was poured into the sediment compartment of the split flow

337

chamber at a matrix temperature of ~38°C. Thereafter, the artificial sediment with microbes

338

was rapidly cooled down to room temperature in the sediment compartment embedding the

339

below-ground tissue of the investigated seagrass specimen (covering the rhizome with

340

artificial sediment to a total depth of ~0.5 cm). The applied pore water was extracted from

341

sediment from the sampling site by means of (i) mild ultrasonication (30 s) in a 50 mL Falcon

342

tube to dissociate microorganisms from the sediment grain surfaces and sediment aggregates

343

(Ramsay, 1984; Lindahl & Bakken, 1995), (ii) centrifugation (2 x 3500g for 5 min at 20°C), and

344

(iii) filtration of supernatants (continuously flushed with N_2 to avoid oxygenation; Millipore®,

345

Polycarbonate membrane filters, 10 µm, USA) to exclude the remaining fine sediment

346

particles.

347

348

ii)   Pre-sterilized below-ground environment (negative control)

349

The below-ground biomass of the investigated seagrasses was surface-sterilized by

350

submerging sediment-free roots and rhizomes in a saline, anoxic ~1.05% (w/v) hypochlorite

351

solution for 30 s (Blaabjerg & Finster, 1998) followed by 3 x 1 min rinses in anoxic, filter-

352

sterilized (0.2 µm) seawater. Prior to casting the sterilized artificial sediment, all added

353

solutions and seawater were filter-sterilized (0.2 µm) and the agar solution was heated to

354

120°C in an oven for 30 min. The sterilized artificial sediment matrix consisted of a ~0.7%

355

(w/v) deoxygenated agar/seawater solution, buffered with sterilized, anoxic HEPES (final

356

concentration of 10 mM: pH 7) and amended with Na_2S to a final H_2S concentration of 500

357

µM (at pH 7); resulting in similar chemical properties to the artificial sediment with added

358

pore water microbes as described above. The transparent, artificial sediment matrix applied

359

360   here permitted the precise and combined application of microsensor measurements and

361   molecular characterisation of microbial communities within specific microzones of interest,

362   *i.e.*, around the basal leaf meristem, root apical meristems and within the bulk sediment.

363

364   *Specimen characteristics and performance*

365   Seagrass specimens with a similar above- to below-ground biomass ratio were selected for

366   this study, to ensure comparable below-ground tissue oxidation capabilities of the

367   investigated specimens (e.g. Frederiksen et al. 2006; Frederiksen & Glud, 2006) (Table S1).

368   The photosynthetic performance of the investigated seagrasses during cultivation was

369   determined as the maximum PSII quantum yield in dark-adapted samples and the effective

370   PSII quantum yield in illuminated samples by means of pulse amplitude modulated (PAM)

371   variable chlorophyll fluorometry (Beer et al. 1998; PocketPAM, equipped with an optical fiber;

372   Gademann Messtechnik GmbH, Germany) (Table S1) to confirm that the seagrasses were

373   generally healthy and photosynthetically active under the experimental conditions (n = 3-7).

374   Following the experiments, the Dry Weight (DW) biomass ratio of the above- to below-ground

375   tissues was obtained after drying each seagrass specimen in an oven at 60°C until a constant

376   weight was reached.

377

378   *Microsensor measurements and flux calculations*

379   We used microsensors to determine the chemical conditions and dynamics at the

380   plant/sediment interface. Clark-type O_2 microsensors (OX-50, Unisense A/S, Aarhus,

381   Denmark; Revsbech, 1989) were used to measure the radial O_2 loss (ROL) from the below-

382   ground tissue of *Zostera muelleri*. The O_2 microsensors were linearly calibrated from signal

383   readings in 100% air saturated seawater and anoxic seawater (obtained by flushing with N_2

384   and adding the O_2 scavenger sodium sulphite) at experimental temperature and salinity. To

385   avoid drifting calibrations during measurements, the O_2 microsensors were pre-contaminated

386   with H_2S before calibrations (Brodersen et al. 2015b). Clark-type H_2S microsensors (H_2S-50,

387   Unisense A/S, Aarhus, Denmark; Jeroschewski et al. 1996; Kühl et al. 1998) were used to

388   measure the H_2S concentration at and around the below-ground tissue of *Zostera muelleri*.

389   The H_2S microsensors were linearly calibrated in acidic (pH 4), anoxic Na_2S solutions of defined

390   H_2S concentrations (0, 50 and 100 µM) at experimental temperature and salinity. pH

391 measurements were performed by means of pH glass microelectrodes (pH-50, Unisense A/S,

392 Aarhus, Denmark; Kühl & Revsbech, 2001) that were used in combination with a reference

393 electrode (REF-RM, Unisense A/S, Aarhus, Denmark) submerged in the split flow chamber to

394 allow the pH microelectrode to develop an electric potential relative to the reference

395 electrode. The pH microelectrodes were linearly calibrated from signal readings in pH buffers

396 (pH 5, 8 and 9) at experimental temperature and salinity.

397

398 Microsensors were mounted on a motorized micromanipulator (MM33-2 & MC-232,

399 Unisense A/S, Aarhus, Denmark) and connected to a microsensor multimeter (Unisense A/S,

400 Aarhus, Denmark) that was interfaced with a PC running dedicated microsensor positioning

401 and data acquisition software (SensorTrace PRO, Unisense A/S, Aarhus, Denmark). The

402 microsensors were carefully positioned at the surface of the basal leaf meristem (defined as

403 0 mm distance from the below-ground tissue on the figures) by manually operating the

404 micromanipulator, while observing the tip of the microsensor relative to the surface of the

405 below-ground tissue through a submerged hand-held lens (described in Brodersen et al. 2014)

406 with a stereo microscope mounted on an articulating arm (SM-6TZ, Amscope, Irvine, CA, USA).

407 All microprofiles were measured in distance increments of 50 μm. Plants were allowed to

408 acclimatize to the experimental conditions for ~72 h before microsensor measurements

409 commenced to ensure steady state geochemical conditions. During microsensor profiling, an

410 additional source of N_2 was immersed into the anoxic seawater layer of the sediment

411 compartment (described above) to avoid O_2 intrusion into the layer and loss of H_2S from the

412 artificial sediment due to oxidation when removing the covering aluminium foil (Brodersen et

413 al. 2014; 2015a,b). Three-to-five microsensor measurements were performed in the artificial

414 sediment at the basal leaf meristem and averaged to produce one replicate microprofile for

415 each of the 2-3 investigated seagrass specimens (*i.e.,* n = 3-5, technical replicates; n = 2-3,

416 biological replicates; which gives a total of 6-15 microsensor profile replicates) in each

417 treatment. Note, that one plant replicate was excluded from the sterilized environment as we

418 could not convincingly determine the below-ground tissue surface during measurements

419 (further described in the supplementary information; Fig. S2).

420

421 **(i)   *Flux calculations***

422 The radial O_2 loss (ROL) from the below-ground tissue (nmol O_2 cm^{-2} h^{-1}) was calculated via a

423 cylindrical version of Fick's first law of diffusion (Steen-Knudsen, 2002) assuming a

424 homogenous, cylinder-shaped O_2 flux from the surface:

425 $$J(r)_{BLM} = \varphi D_0 (C_1 - C_2)/r ln(\frac{r_1}{r_2})$$

426 where φ is the porosity of the artificial sediment (here assumed to be similar to seawater); D_0

427 is the molecular diffusion coefficient of O_2 in seawater at experimental temperature and

428 salinity; r is the radius of the basal leaf meristem; and C_1 and C_2 are the O_2 concentrations

429 measured at the radial distances r_1 and r_2 from the tissue surface, respectively. The H_2S

430 oxidation rates in the immediate rhizosphere (nmol H_2S cm^{-2} h^{-1}) were calculated in a similar

431 manner by correcting D_0 to the molecular diffusion coefficient for H_2S at experimental

432 temperature and salinity (factor 0.7573; tabulated values are accessible on

433 www.unisense.com).

434

435 The following equations where used to calculate the total sulphide concentration

436 microprofiles and fluxes from the measured H_2S concentrations and pH microprofiles

437 (equations are available at www.unisense.com):

438 $$pK_1 = -98.08 + \frac{5765.4}{T} + 15.04555 \times \text{LN(T)} + \left(-0.157 \times (S^{0.5})\right) + 0.0135 \times S$$

439 where *S* is the salinity and *T* is the temperature in Kelvin.

440 $$total\ sulphide\ [S_{tot}{}^{2-}] = [H_2S] \times (1 + \frac{K_1}{[H_3O^+]})$$

441 where *$[H_3O^+]$ = $[H^+]$ = 10^{-pH}* and *K_1 = 10^{-pK1}*; for pH < 9 (Jeroschewski et al. 1996).

442

443 *Sediment sampling for DNA extractions*

444 Artificial sediment samples were obtained from selected regions of interest, i.e., around the

445 basal leaf meristem (BLM; at the root/shoot junction), around the root apical meristem (RAM;

446 at the root-tip), and from the bulk sediment (BS) using a sterilized surgical knife and spatula

447 (Fig. S6). Samples around the below-ground tissues were carefully collected at a radial

448 distance of up to ~1 mm from the tissue surface (final volume of ~100 µL). Only one sediment

449 sample was acquired from each of the meristem areas (i.e., the BLM and the RAM) of the

450 three investigated seagrass plants cultured in artificial sediment enriched with native

451 porewater microbes, as we were only interested in the small volume of sediment affected by

452   the plant (n = 3). Whereas several samples (or large sediment volumes) were obtained from

453   the bulk artificial sediment area (n = 3-4); taken from both the porewater enriched and pre-

454   sterilized (here used as a microbial negative control) treatments. After sampling, the sediment

455   samples were stored in 2 mL Eppendorf tubes in a -80°C freezer until further analysis. Prior to

456   DNA extraction, four rounds of washing were performed in order to remove the agarose. The

457   artificial sediment samples were first liquefied in a dry bath at ~50°C and were then

458   subsequently diluted via centrifugation with 1 mL of 3x PBS (2x 7500g at room temperature

459   for 10 min, followed by 2x 4000g at 40°C for 10 min; all after re-heating the sample/PBS

460   mixture to ~45°C). This additional cleaning step was implemented to separate bacterial cells

461   from the agarose medium.

462

463   *DNA extraction and PCR sequencing*

464   A modified phenol:chloroform DNA extraction protocol was employed to extract microbial

465   DNA from the artificial sediment matrix. We added 600 μL lysis buffer (TE buffer pH 8, 0.5%

466   SDS, 0.1 mg mL^{-1}) to the pellets prior to incubation at 37°C for 1 h. Then 100 μL of 5 M NaCl,

467   and 80 μL of 10% CTAB were added and the mixture was incubated at 65°C for 10 min. Lysates

468   were transferred to sterile tubes and DNA was extracted following standard

469   phenol:chloroform procedures (Zhou et al. 1996). The obtained DNA was air-dried,

470   resuspended in 20 μL of dH$_2$O and stored at -20°C until further analysis. DNA quantity and

471   purity was evaluated using a Nanodrop-1000 Spectrophotometer (NanoDrop 1000; Thermo

472   Scientific, USA).

473

474   **(i)   PCR amplification and sequencing**

475   To track shifts in the overall composition of the bacterial community, 16S rRNA amplicon

476   sequencing was performed. Amplicons of variable regions V1-V3 of the 16S rRNA gene,

477   generated using the primers 27F (5'-AGAGTTTGATCMTGGCTCAG-3') (Weinbauer et al. 2002)

478   and 519R (5'-GWATTACCGCGGCKGCTG-3') (Lane, 1991; Turner et al., 1999), were sequenced

479   on the Illumina MiSeq platform (Molecular Research LP; Shallowater, TX, USA) following the

480   manufacturer's guidelines. Bacterial 16S rRNA gene sequences were analysed using the QIIME

481   pipeline (Caporaso et al., 2010; Kuczynski et al., 2012). Briefly, paired-end DNA sequences

482   were joined, *de novo* Operational Taxonomic Units (OTUs) were defined at 97% of sequences,

483   and identity was assigned against the Greengenes database (version 13/8/2013) using BLAST

484   (Altschul et al., 1990). Chimeric sequences were detected using ChimeraSlayer (Haas et al.,

485   2011) and filtered out from the dataset. Chloroplasts and mitochondrial reads were removed

486   before downstream analysis. Sequences were then rarefied to the same depth (7265

487   sequences per sample) to remove the effect of sampling effort upon analysis. Raw data files

488   in FASTQ format were deposited in the NCBI Sequence Read Archive (SRA) with the study

489   accession number SRP073850 under Bioproject number PRJNA315465.

490

491   *Statistical analysis*

492   Data were tested for equal variance prior to statistical analysis. Student's *t*-tests were used

493   to compare relative microbial abundances between the different regions of interest (i.e. RAM,

494   BLM and BS).

495

503

504 **SUPPLEMENTARY INFORMATION**

505 Supplementary Information accompanies the paper on the Environmental Microbiology

506 website (http://onlinelibrary.wiley.com/journal/10.1111/(ISSN)1462-2920).

507 **Figure S1.** Chemical microenvironment as measured with microsensors at the surface of the
508 basal leaf meristem of *Zostera muelleri* maintained in (i) a pre-sterilized environment and (ii)
509 with added native pore water microbes – plant 2.

510 **Figure S2.** Chemical microenvironment as measured with microsensors at the surface of the
511 basal leaf meristem of *Zostera muelleri* maintained in reduced, artificial sediment with added
512 native pore water microbes – plant 3.

513 **Figure S3.** Total sulphide concentration microprofiles at the surface of the basal leaf meristem
514 of *Zostera muelleri* maintained in (i) a pre-sterilized environment and (ii) with added native
515 pore water microbes – plant 1.

516 **Figure S4.** Total sulphide concentration microprofiles at the surface of the basal leaf meristem
517 of *Zostera muelleri* maintained in (i) a pre-sterilized environment and (ii) with added native
518 pore water microbes – plant 2.

519 **Figure S5.** Principal component analysis plot of the rhizosphere microbial community
520 composition, illustrating the separation of the microbial consortia within selected
521 rhizospheric regions of interest.

522 **Figure S6.** Conceptual diagram visualizing sampling areas (i.e. region of interests) within the
523 reduced, artificial sediment.

524 **Table S1.** Photosynthetic parameters as measured by variable chlorophyll fluorescence and
525 measures of the above-ground:below-ground biomass ratios.

526

527

528 **CONFLICT OF INTEREST STATEMENT**

529 The authors declare that the research was conducted in the absence of any commercial or

530 financial relationships that could be construed as a potential conflict of interest.

531

532 **FIGURE LEGENDS**

533 **Figure 1**. The below-ground chemical microenvironment at the basal leaf meristem, i.e., the
534 meristematic region of the rhizome of the seagrass *Zostera muelleri*. (a) and (b) represent
535 microsensor measurements in an artificial sediment matrix with added pore water microbes.
536 (c) and (d) represent microsensor measurements in a pre-sterilized environment, i.e.,
537 sterilized artificial sediment matrix and below-ground tissue surface. (a) and (c) show
538 measurements in darkness. (b) and (d) show measurements in light (photon irradiance of
539 ~150 μmol photons m^{-2} s^{-1}). Black line and symbols show the O$_2$ concentration; Red line and
540 symbols show the H$_2$S concentration; Blue line and symbols show pH. The dotted lines
541 indicate the thickness of the plant-derived oxic microzone, and X = 0 indicates the surface of
542 the basal leaf meristem. Symbols with error bars represent means ± S.D (n = 3-4 technical
543 replicates; biological replication of the below-ground chemical microenvironment dynamics
544 is shown in the Supplementary Results; Fig. S1 and S2).

545 **Figure 2.** Microbial diversity in the rhizosphere of the seagrass *Zostera muelleri* determined
546 via 16S rRNA amplicon sequencing. The phylogenetic tree denotes the spatial separation of
547 the microbial consortia as determined via beta diversity analysis by Jackknife comparison of
548 the weighted sequences data. The heat-map shows the abundance of the respective bacterial
549 class/genus within the selected regions of interest, where (o) and (f) denote order and family
550 classification, respectively. The heat-map includes taxonomic groups within each sample that
551 represent >1% of the total sequences, which cumulatively represents >85% of the total
552 sequenced data. Diagrams (in %) show the mean relative abundance of designated bacterial
553 classes present within the selected regions of interest of the artificial sediment matrix. All
554 data originate from reduced, artificial sediment with added native pore water microbes
555 (except from data given for the negative control, which originates from a pre-sterilized
556 environment as described in the Experimental procedures section). n = 2-3.

557

558   **REFERENCE LIST**

559   Altschul, S.F., Gish, W., Miller, W., Myers, E.W., and Lipman, D.J. (1990) Basic local alignment
560   search tool. *Journal of molecular biology* **215**: 403-410.

561   Barnabas, A.D. (1996) Casparian band-like structures in the root hypodermis of some aquatic
562   angiosperms. *Aquatic Botany* **55**: 217-225.

563   Beer, S., Vilenkin, B., Weil, A., Veste, M., Susel, L., and Eshel, A. (1998) Measuring
564   photosynthetic rates in seagrasses by pulse amplitude modulated (PAM) fluorometry.
565   *Marine Ecology Progress Series* **174**: 293-300.

566   Blaabjerg, V., and Finster, K. (1998) Sulphate reduction associated with roots and rhizomes of
567   the marine macrophyte *Zostera marina*. *Aquatic Microbial Ecology* **15**(3): 311-314.

568   Blaabjerg, V., Mouritsen, K.N., and Finster, K. (1998) Diel cycles of sulphate reduction rates in
569   sediments of a *Zostera marina* bed (Denmark). *Aquatic Microbial Ecology* **15**(1): 97-
570   102.

571   Borum, J., Pedersen, O., Greve, T.M., Frankovich, T.A., Zieman, J.C., Fourqurean, J.W., *et al*.
572   (2005) The potential role of plant oxygen and sulphide dynamics in die-off events of
573   the tropical seagrass, *Thalassia testudinum*. *Journal of Ecology* **93**: 148-158.

574   Borum, J., Sand-Jensen, K., Binzer, T., Pedersen, O., and Greve, T. (2006) Oxygen movement
575   in seagrasses. In Larkum AWD, Orth JR & Duarte CM, Eds., *Seagrasses: Biology, Ecology*
576   *and Conservation*, Dordrecht, The Netherlands. Springer, Berlin: 255-270.

577   Brodersen, K.E., Koren, K., Lichtenberg, M., and Kühl, M. (2016) Nanoparticle-based
578   measurements of pH and O_2 dynamics in the rhizosphere of *Zostera marina* L.: Effects
579   of temperature elevation and light/dark transitions. *Plant, Cell & Environment* **39**:
580   1619-1630.

581   Brodersen, K.E., Koren, K., Moßhammer, M., Ralph, P.J., Kühl, M., and Santner, J. (2017)
582   Seagrass-mediated phosphorus and iron solubilization in tropical sediments.
583   *Environmental Science & Technology* **51**: 14155-14163.

584   Brodersen, K.E., Lichtenberg, M., Paz, L.-C., and Kühl, M. (2015b) Epiphyte-cover on seagrass
585   (*Zostera marina* L.) leaves impedes plant performance and radial O_2 loss from the
586   below-ground tissue. *Frontiers in Marine Science* **2**: 58.

587   Brodersen, K.E., Nielsen, D.A., Ralph, P.J., and Kühl, M. (2014) A split flow chamber with
588   artificial sediment to examine the below-ground microenvironment of aquatic
589   macrophytes. *Marine Biology* **161**(12): 2921-2930.

590   Brodersen, K.E., Nielsen, D.A., Ralph, P.J., and Kühl, M. (2015a) Oxic microshield and local pH
591   enhancement protects *Zostera muelleri* from sediment derived hydrogen sulphide.
592   *New Phytologist* **205**: 1264-1276.

593   Caporaso, J.G., Kuczynski, J., Stombaugh, J., Bittinger, K., Bushman, F.D., Costello, E.K., *et al*.
594   (2010) QIIME allows analysis of high-throughput community sequencing data. *Nature*
595   *Methods* **7:** 335-336.

596   Colmer, T.D. (2003) Long-distance transport of gases in plants: a perspective on internal
597   aeration and radial oxygen loss from roots. *Plant, Cell & Environment* **26**: 17-36.

598   Costanza, R., d'Arge, R., de Groot, R., Farber, S., Grasso, M., Hannon, B., *et al*. (1997) The value
599   of the world's ecosystem services and natural capital. *Nature* **387**: 253-260.

600   Cúcio, C., Engelen, A.H., Costa, R., and Muyzer, G. (2016) Rhizosphere microbiomes of
601   European seagrasses are selected by the plant, but are not species specific. *Frontiers*
602   *in Microbiology* **7**: 440.

603   Devereux, R. (2005) Seagrass rhizosphere microbial communities. In *Coastal and estuarine*
604   *studies: Interactions between macro- and microorganisms in marine sediments*,
605   editors: Erik Kristensen, Ralf R. Haese & Joel E. Kostka. American Geophysical Union.
606   Washington, USA.

607   Duarte, C.M., Middelburg, J., and Caraco, N. (2005) Major role of marine vegetation on the
608   oceanic carbon cycle. *Biogeosciences* **2**: 1–8.

609   Ettinger, C.L., Voerman, S.E., Lang, J.M., Stachowicz, J.J., Eisen, J.A. (2017) Microbial
610   communities in sediment from *Zostera marina* patches, but not the *Z. marina* leaf or
611   root microbiomes, vary in relation to distance from patch edge. *PeerJ* 5: e3246

612   Fahimipour, A.K., Kardish, M.R., Lang, J.M., Green, J.L., Eisen, J.A., and Stachowicz, J.J. (2017)
613   Global-scale structure of the eelgrass microbiome. *Applied and Environmental*
614   *Microbiology*.   Accepted   manuscript   posted   online   April   14,   2017.
615   doi:10.1128/AEM.03391-16

616   Fourqurean, J.W., Duarte, C.M., Kennedy, H., Marba, N., Holmer, M., Mateo, M.A., *et al*.
617   (2012) Seagrass ecosystems as a globally significant carbon stock. *Nature Geoscience*
618   **5**: 505-509.

619   Frederiksen, M.S., and Glud, R.N. (2006) Oxygen dynamics in the rhizosphere of *Zostera*
620   *marina*: A two-dimensional planar optode study. *Limnology and Oceanography* **51**(2):
621   1072-1083.

622 Frederiksen, M.S., Holmer, M., Borum, J., and Kennedy, H. (2006) Temporal and spatial
623   variation of sulfide invasion in eelgrass (*Zostera marina*) as reflected by its sulfur
624   isotopic composition. *Limnology and Oceanography* **51**(5): 2308-2318.

625 Haas, B.J., Gevers, D., Earl, A.M., Feldgarden, M., Ward, D.V., Giannoukos, G., *et al*. (2011)
626   Chimeric 16S rRNA sequence formation and detection in Sanger and 454-
627   pyrosequenced PCR amplicons. *Genome research* **21**: 494-504.

628 Hansen, J.W., Udy, J.W., Perry, C.J., Dennison, W.C., and Lomstein, B.A. (2000) Effect of the
629   seagrass *Zostera capricorni* on sediment microbial processes. *Marine Ecology Progress
630   Series* **199**: 83-96.

631 Harborne, A.R., Mumby, P.J., Micheli, F., Perry, C.T., Dahlgren, C.P., Holmes, K.E., *et al*. (2006)
632   The functional value of Caribbean coral reef, seagrass and mangrove habitats to
633   ecosystem processes. *Advances in Marine Biology* **50**: 57-189.

634 Holmer, M., Pedersen, O., and Ikejima, K. (2006) Sulfur cycling and sulfide intrusion in mixed
635   Southeast Asian tropical seagrass meadows. *Botanica Marina* **49**: 91-102.

636 Isaksen, M.F., and Finster, K. (1996) Sulphate reduction in the root zone of the seagrass
637   *Zostera noltii* on the intertidal flats of a coastal lagoon (Arcachon, France). *Marine
638   Ecology Progress Series* **137**(1): 187-194.

639 Jensen, S.I., Kühl, M., Glud, R.N., Jørgensen, L.B., and Prieme, A. (2005) Oxic microzones and
640   radial oxygen loss from roots of *Zostera marina*. *Marine Ecology Progress Series* **293**:
641   49-58.

642 Jensen, S.I., Kühl, M., and Prieme, A. (2007) Different bacterial communities in the rhizoplane
643   and bulk sediment of the seagrass *Zostera marina*. *FEMS Microbiology Ecology* **62**:
644   108-117.

645 Jeroschewski, P., Steuckart, C., and Kühl, M. (1996) An amperometric microsensor for the
646   determination of H_2S in aquatic environments. *Analytical Chemistry* **68**: 4351-4357.

647 Jørgensen, B.B. (1982) Mineralization of organic matter in the sea bed - the role of sulphate
648   reduction. *Nature* **296**: 643-645.

649 Jørgensen, B.B., and Revsbech, N.P. (1983) Colorless sulfur bacteria, *Beggiatoa* spp. and
650   *Thiovulum* spp., in O_2 and H_2S microgradients. *Applied and Environmental
651   Microbiology* **45**: 1261-1270.

652 Koren, K., Brodersen, K.E., Jakobsen, S.L., and Kühl, M. (2015) Optical sensor nanoparticles in
653   artificial sediments – a new tool to visualize O_2 dynamics around the rhizome and roots
654   of seagrasses. *Environmental Science and Technology* **49**(4): 2286-2292.

655   Kuczynski, J., Stombaugh, J., Walters, W.A., González, A., Caporaso, J.G., and Knight, R. (2012)
656   Using QIIME to analyze 16S rRNA gene sequences from microbial communities.
657   *Current protocols in microbiology*, 1E. 5.1-1E. 5.20.

658   Kühl, M., and Revsbech, N.P. (2001) Biogeochemical microsensors for boundary layer studies.
659   In Boudreau, B.P., Jørgensen, B.B., eds. *The Benthic Boundary Layer*. Oxford University
660   Press, New York, 180-210.

661   Kühl, M., Steuckart, C., Eickert, G., and Jeroschewski, P. (1998) A H_2S microsensor for profiling
662   sediments and biofilms: Application in acidic sediment. *Aquatic Microbial Ecology* **15**:
663   201-209.

664   Larkum, A.W.D., Orth, R.J., and Duarte, C.M. (2006) *Seagrasses: Biology, Ecology and*
665   *Conservation*. Springer, Berlin, Printed in Dordrecht, The Netherlands.

666   Lamers, L.P., Govers, L.L., Janssen, I.C., Geurts, J.J., Van der Welle, M.E., Van Katwijk, M.M., *et*
667   *al*. (2013) Sulfide as a soil phytotoxin—a review. *Frontiers in Plant Science* **4**: 268.

668   Lane, D. (1991) 16S/23S rRNA sequencing. In *Nucleic acid techniques in bacterial systematics*
669   (Stackebrandt, E., and Goodfellow, M., eds.). New York, NY. John Wiley and Sons: 125-
670   175.

671   Lindahl, V., and Bakken, L.R. (1995) Evaluation of methods for extraction of bacteria from soil.
672   *FEMS Microbiology Ecology* **16**(2): 135-142.

673   Madsen, J.D., Chambers, P.A., James, W.F., Koch, E.W., and Westlake, D.F. (2001) The
674   interaction between water movement, sediment dynamics and submersed
675   macrophytes. *Hydrobiologia* **444**(1-3): 71-84.

676   Moriarty, D.J.W., Iverson, R.L., and Pollard, P.C. (1986) Exudation of organic carbon by the
677   seagrass *Halodule wrightii* Aschers. and its effect on bacterial growth in the sediment.
678   *Journal of Experimental Marine Biology and Ecology* **96**(2): 115-126.

679   Nelson, D.C., Jørgensen, B.B., and Revsbech, N.P. (1986) Growth pattern and yield of a
680   chemoautotrophic *Beggiatoa sp.* in oxygen-sulfide microgradients. *Applied and*
681   *Environmental Microbiology* **52**(2): 225-233.

682   Nielsen, L.B., Finster, K., Welsh, D.T., Donelly, A., Herbert, R.A., De Wit, R., *et al*. (2001)
683   Sulphate reduction and nitrogen fixation rates associated with roots, rhizomes and
684   sediments from *Zostera noltii* and *Spartina maritima* meadows. *Environmental*
685   *Microbiology* **3**(1): 63-71.

686   Nielsen, A.H., Vollertsen, J., and Hvitved-Jacobsen, T. (2006) Kinetics and stoichiometry of
687   aerobic sulfide oxidation in wastewater from sewers - effects of pH and temperature.
688   *Water Environment Research* **78**: 275-283.

689 Pagès, A., Teasdale, P.R., Robertson, D., Bennett, W.W., Schäfer, J., and Welsh, D.T. (2011)
690   Representative measurement of two-dimensional reactive phosphate distributions
691   and co-distributed iron(II) and sulfide in seagrass sediment porewaters. *Chemosphere*
692   **85**(8): 1256-1261.

693 Pagès, A., Welsh, D.T., Robertson, D., Panther, J.G., Schäfer, J., Tomlinson, R.B., *et al*. (2012)
694   Diurnal shifts in co-distributions of sulfide and iron(II) and profiles of phosphate and
695   ammonium in the rhizosphere of *Zostera capricorni*. *Estuarine, Coastal and Shelf*
696   *Science* **115**: 282-290.

697 Pedersen, O., Binzer, T., and Borum, J. (2004) Sulphide intrusion in eelgrass (*Zostera marina*
698   L.). *Plant, Cell and Environment* **27**: 595-602.

699 Pedersen, O., Borum, J., Duarte, C.M., and Fortes, M.D. (1998) Oxygen dynamics in the
700   rhizosphere of *Cymodocea rotundata*. *Marine Ecology Progress Series* **169**: 283-288.

701 Pollard, P.C., and Moriarty, D.J.W. (1991) Organic carbon decomposition, primary and
702   bacterial productivity, and sulphate reduction, in tropical seagrass beds of the Gulf of
703   Carpentaria, Australia. *Marine Ecology Progress Series* **69**(1): 149-159.

704 Ramsay, A.J. (1984) Extraction of bacteria from soil: efficiency of shaking or ultrasonication as
705   indicated by direct counts and autoradiography. *Soil biology and biochemistry* **16**(5):
706   475-481.

707 Revsbech, N.P. (1989) An oxygen microsensor with a guard cathode. *Limnology and*
708   *Oceanography* **34**(2): 474-478.

709 Sallam, A., and Steinbüchel, A. (2009) *Clostridium sulfidigenes* sp. nov., a mesophilic,
710   proteolytic, thiosulfate- and sulfur-reducing bacterium isolated from pond sediment.
711   *International Journal of Systematic and Evolutionary Microbiology* **59**(7): 1661-1665.

712 Steen-Knudsen, O. (2002) *Biological membranes: Theory of Transport, Potentials and Electric*
713   *Impulses*. Cambridge: Cambridge University Press.

714 Thomas, F., Hehemann, J.-H., Rebuffet, E., Czjzek, M., and Michel, G. (2011) Environmental
715   and gut Bacteroidetes: the food connection. *Frontiers in Microbiology* **2**: 93.

716 Turner, S., Pryer, K., Miao, V., and Palmer, J. (1999) Investigating deep phylogenetic
717   relationships among cyanobacteria and plastids by small subunit rRNA sequence
718   analysis. *Journal of Eukaryotic Microbiology* **46**: 327-338.

719 van der Heide, T., Govers, L.L., de Fouw, J., Olff, H., van der Geest, M., van Katwijk, M.M., *et*
720   *al*. (2012) A Three-Stage Symbiosis Forms the Foundation of Seagrass Ecosystems.
721   *Science* **336**: 1432-1434.

722   Ward, L.G., Kemp, W.M., and Boynton, W.R. (1984) The influence of waves and seagrass
723   communities on suspended particulates in an estuarine embayment. *Marine Geology*
724   **59**: 85-103.

725   Weinbauer, M.G., Fritz, I., Wenderoth, D.F., and Höfle, M.G. (2002) Simultaneous extraction
726   from bacterioplankton of total RNA and DNA suitable for quantitative structure and
727   function analyses. *Applied and Environmental Microbiology* **68**(3): 1082-1087.

728   Welsh, D.T. (2000) Nitrogen fixation in seagrass meadows: regulation, plant–bacteria
729   interactions and significance to primary productivity. *Ecology Letters* **3**(1): 58-71.

730   Wesley, L.D. (2009) Fundamentals of soil mechanics for sedimentary and residual soils. *John
731   Wiley & Sons.*

732   York, P.H., Smith, T.M., Coles, R.G., McKenna, S.A., Connolly, R.M., Irving, A.D., *et al*. (2016)
733   Identifying knowledge gaps in seagrass research and management: an Australian
734   perspective. *Marine Environmental Research*. (accepted on June 10, 2016)

735   Zhou, J., Bruns, M.A., and Tiedje, J.M. (1996) DNA recovery from soils of diverse composition.
736   *Applied and Environmental Microbiology* **62**: 316-322.

737

738   **Figures**

739

DARK   LIGHT

740

741   **Fig. 1**

742

743

Fig. 2

744

745

746

747

748
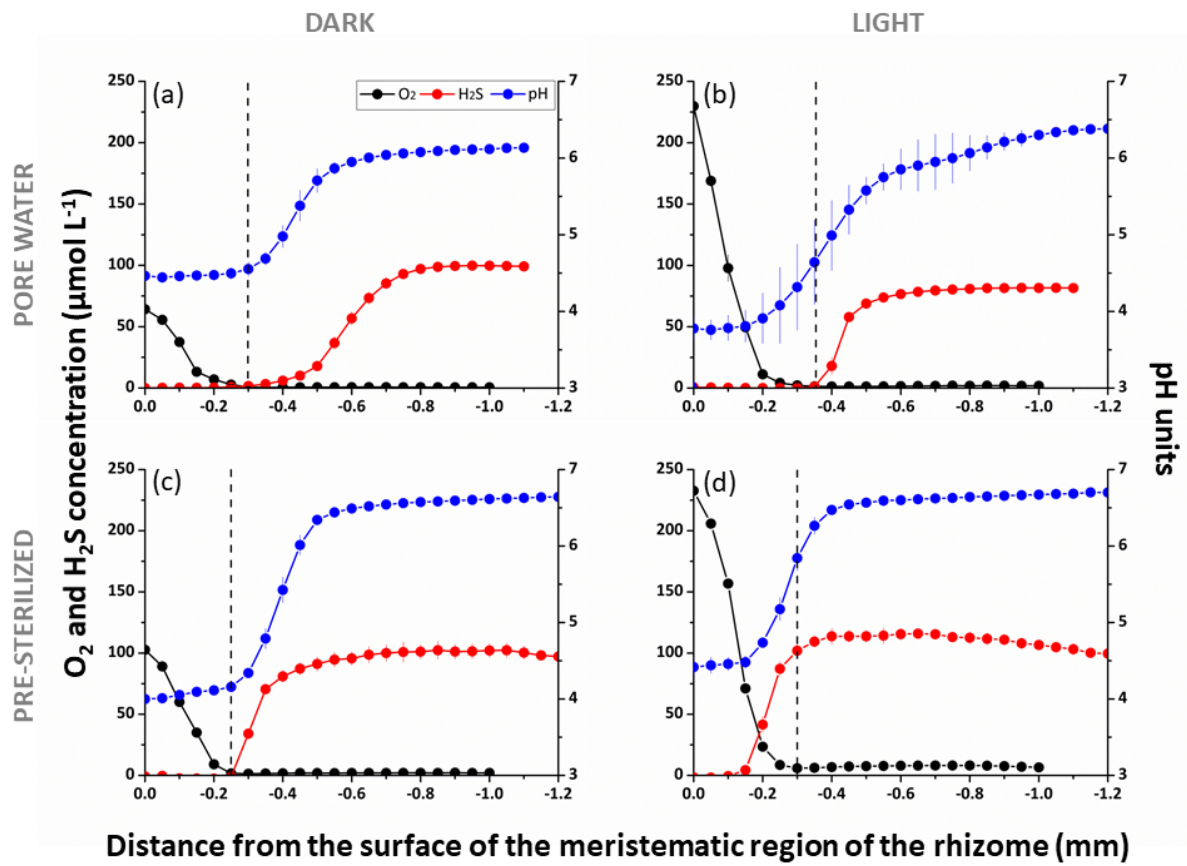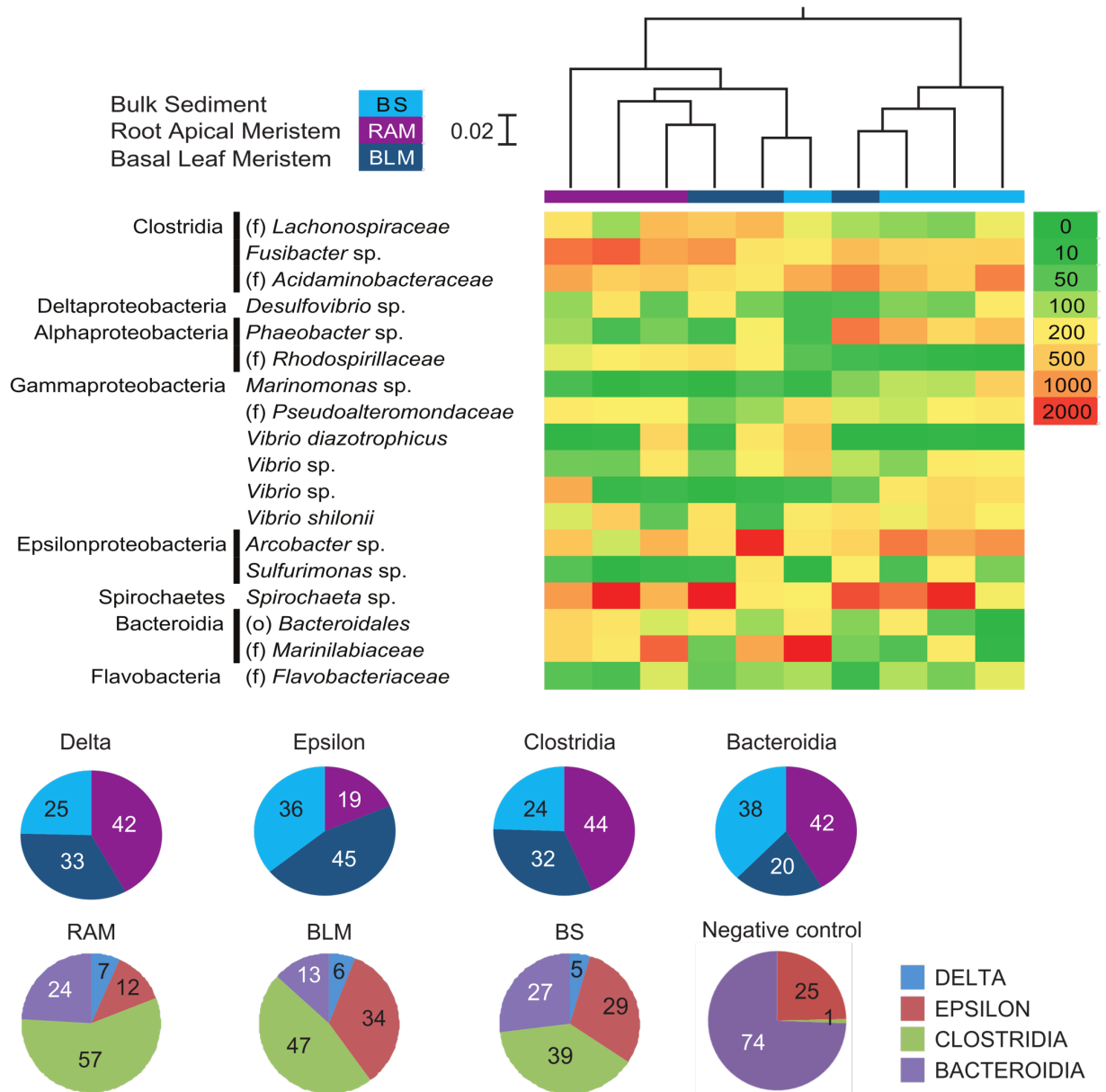
749 **Tables**

750

751 **Table 1.** Radial O_2 loss (ROL), plant-derived H_2S re-oxidation/sediment detoxification and ΔpH in the
752 immediate rhizosphere of *Z. muelleri*.

	ROL nmol O_2 cm^{-2} h^{-1}	H_2S re-oxidation nmol H_2S cm^{-2} h^{-1}	S_{tot}^{2-} oxidation nmol S_{tot}^{2-} cm^{-2} h^{-1}	ΔpH pH units
pore water				
dark	-322 ± 39	334 ± 1	555 ± 164[a]	2.1 ± 0.4[a]
light	-745 ± 118	418 ± 4	440 ± 6	2.4 ± 0.2
pre-sterilized				
dark	-378 ± 3	636 ± 136[a]	651 ± 146[a]	2.5 ± 0.1
light	-891 ± 52	508 ± 33	533 ± 22	2.5 ± 0.2

753 n = 2-3, biological replication. Values are mean ± S.E.M. *Pore water* indicate artificial sediment matrix
754 with added native pore water microbes. *Pre-sterilized* indicate a sterilized below-ground environment,
755 i.e., sterilized sediment and below-ground biomass. S_{tot}^{2-} = total sulphide. [a]Note relative high standard
756 error of the mean (S.E.M.).

757

758